Optoelectronics Using 2D Colloidal Nanocrystals from Wide Band Gap to Narrow Band Gap Materials

Bertille Martinez, Clément Livache, Nicolas Goubet, Eva Izquierdo, Mathieu G. Silly, Sandrine Ithurria, Emmanuel Lhuillier

Optoelectronics using 2D colloidal nanocrystals from wide band gap to narrow band gap materials

Bertille Martinez[1,2], Clément Livache[1,2], Nicolas Goubet[1,2], Eva Izquierdo[2], Mathieu G Silly[3], Sandrine Ithurria[2], Emmanuel Lhuillier[1*]

[1] Sorbonne Universités, UPMC Univ Paris 06, CNRS-UMR 7588, Institut des NanoSciences de Paris, 4 place Jussieu, 75005 Paris, France

[2] Laboratoire de Physique et d'Etude des Matériaux, ESPCI Paris, PSL Research University, Sorbonne Université UPMC Univ Paris 06, CNRS, 10 rue Vauquelin 75005 Paris, France.

[3]Synchrotron-SOLEIL, Saint-Aubin, BP48, F91192 Gif sur Yvette Cedex, France

Abstract: Colloidal nanocrystals are playing an increasing role for the development of low cost optoelectronics. Among these materials, 2D nanoplatelets (NPL) offer particularly well controlled optical features and their integration into device such as transistor and photoconductor is here discussed. We present recent results obtained on the optoelectronic properties of CdSe/CdS and HgTe 2D nanoplatelets (NPL). The manuscripts is organized along three main sections. The first part is an introduction to 2D NPLs and their structural and optical properties. The second part get focused on CdSe/CdS NPL and their photoconductive properties. We in particular highlight the key role plays by the 2D geometries on the charge dissociation. Finally the last part of the paper discusses about the recent report of HgTe and HgSe NPL with optical features in the near infrared. Here we discuss how the surface chemistry can be used to tune the majority carrier and the photoconductive properties of the material.

Keywords: nanocrystals, 2D nanoplatelets, optoelectronics, conduction and photoconduction

*To whom correspondence should be addressed. E-mail: el@insp.upmc.fr

Introduction

In the field of colloidal nanocrystals, 2D nanoplatelets [1,2] (NPL) are a special class of nanoparticles with especially well controlled optical features. NPL present a lateral extension above the material Bohr radius, while their thickness is quite thin and leads to quantum confinement in this only direction (electron microscopy images of the platelets are provided on Figure 1a). They have been reported with a broad range of materials including cadmium chalcogenides [3,4,5], lead chalcogenides [6,7], indium selenide [8] and more recently even using perovskites of $CsPbX_3$ [9]. In the case of II-VI materials, the growth mechanism [10] is leading to a complete absence of roughness along the thickness direction. As a result, the absorption edge and photoluminescence (PL) signal are respectively sharp and narrow, see Figure 1b. Typically, the PL linewidth is three times narrower than the value reported for CdSe spherical objects at the same emitting wavelength.

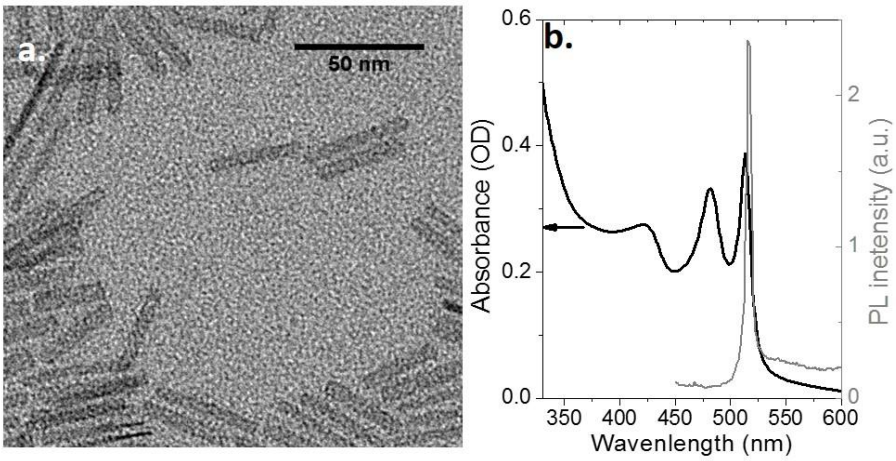

Figure 1 a: TEM image of CdSe nanoplatelets. b: Absorption and photoluminescence spectra of CdSe nanoplatelets.

In addition to conventional core-shell structures [11,12], the 2D geometry allows the growth of heterostructure in a geometry which was not possible with 0D objects: the core crown system [13,14]. Even more complex combination, such as core crown shell, has recently been demonstrated [15].

In addition to their narrow excitonic features, NPL present fast PL emission which makes them appealing for light emission: they have led to low lasing threshold properties both in single [16,17] and two photon [18] pumping configuration. On the other hand, their transport properties remain far less investigated [8,19,20,21]. In this short review, we present the transport and phototransport properties of CdSe/CdS NPL and how their dimensionality impacts their properties. In the second part of the manuscript, we discuss how to expand the exceptional properties of cadmium chalcogenides to other narrower band gap systems such as mercury chalcogenides.

Conduction and photoconduction in wide band gap nanoplatelets

Because of their anisotropic shape, the transport in NPL solid films raises great expectation to achieve large mobility films. Indeed, in nanocrystal films, electronic transport occurs through a hopping process. Around room temperature, transport is limited to the closest neighbor, and so the carriers have to hop

from one nanoparticle to the other using tunneling effect to reach electrodes. In most devices based on planar geometry, the spacing between electrodes is a few μm, while the particle size is a few nm, which makes that a thousand hopping step are typically necessary to go from one electrode to the other. By using larger object like nanoplatelets, the number of hopping steps and thus the number of tunnel events should be reduced. In the following, we focus on CdSe/CdS NPL because of their stable properties over time.

To make the NPL film conductive, we first exchange the capping ligand at the surface of the NPL toward S^{2-} capping [22] using a phase transfer method, which leads to a more complete ligand exchange compared to solid state approach of the ligand exchange. As light is shone on the film, the conductance rises but the overall responsivity of the film remains weak in the tens of $\mu A.W^{-1}$ range [23,24]. This limited performance results from the fact that photogenerated electrons are quickly trapped on shallow trap states [25] in the vicinity of the conduction band [26]. As a result, the necessary time for the electron to reach the electrodes is long and the associated gain (defined as the ratio of the transit time over the minority carrier lifetime) is weak.

From photoconduction to phototransistor

To overcome this issue, we develop an electrolyte gating approach of the NPL film [26,27]. The method consists in brushing an almost solid ion gel made of high molar weight polyethylene glycol matrix containing $LiClO_4$ ions. The method presents several advantages: (i) being air operable, (ii) it can be applied with a broad range of metal chalcogenides (CdSe, CdS, CdTe, HgS, HgTe, HgSe, PbS, PbSe…), (iii) it presents a large gate capacitance which allows to tune up the doping to several carriers per nanocrystals [28]. By applying a gate bias, we observe a large tunability of the drain source conductance, see Figure 2a. As holes are injected (negative gate bias), the system remains in an insulating state; on the other hand, if electrons are injected the conductance rises by almost 9 orders of magnitude. This means that the nanoplatelets are behaving as an *n*-type material, which is consistent with photoemission measurements [29].

As a gate bias is applied, not only we observe a strong tunability of the dark current but the photoresponse is also affected, see Figure 2b. At low gate bias, a similar behavior to purely photoconductive film without gate is observed. The photoresponse is weak and the cut off frequency is above 100 kHz. When the bias is increased, the photoresponse rises and this increase can reach up to several orders of magnitude. Actually this rise of the photoconductance results from the filling by the gate of the shallow traps below the conduction band. As a result, photogenerated carriers can spend time in the conduction band rather than in the traps: the transit time is higher, which leads to a stronger gain.

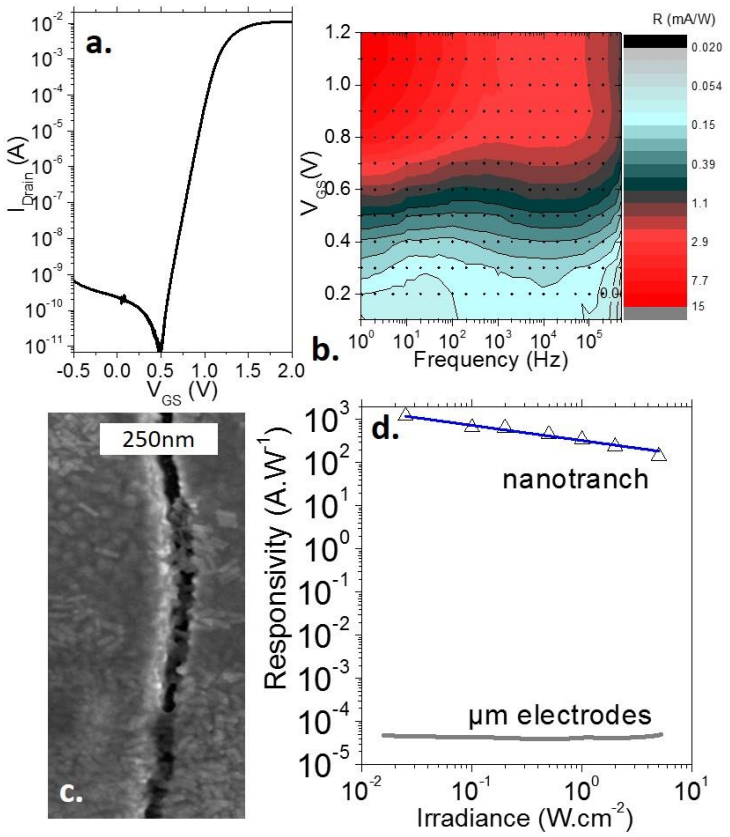

Figure 2a: Transfer curve (drain current vs *gate bias) for a film of CdSe/CdS NPL. b: Responsivity map of a film of CdSe/CdS NPL as a function of illumination frequency and gate bias. c: SEM image of a nanotrench coated with the CdSe/CdS NPL. d: Responsivity as a function of the light irradiance for a film of CdSe/CdS NPL deposited on µm spaced electrodes (grey) or on a nanotrench (blue).*

Impact of the large binding energy observed with 2D objects.

One key question which remains unaddressed in the previous devices [23,30] is the large exciton binding energy observed for 2D objects [31,32]. Indeed for a given material, as we switch from 0D object to 2D object, the electron-hole pair binding energy is increased by a factor 10, to reach 200 – 300 meV for CdSe NPL. This value is actually closer to the reported values for 2D transition metal dichalcogenides for which the binding energy can be as high as 0.5 or even 1 eV.

As a result, a large electric field needs to be applied over the NPL to overcome the coulombic binding of the electron-hole pair. To do so, we use nanotrench electrodes [33] which are two electrodes spaced by few tens of nm. The latter presents the key advantage to be fairly simple to build by using two steps of optical lithography [27] in spite of the very subwavelength character of the device. The spacing of the electrodes is chosen to fit with the lateral extension of the NPL, see Figure 2c. The effect on the photoresponse is absolutely dramatic and we observe a 10^7 enhancement of the responsivity, see Figure 2d. This magnification results from the combination of three effects: (i) a more efficient charge dissociation because of the higher electric field, (ii) a change in the transport mechanism which switches from hopping

to a single tunnel event and finally (iii) the short spacing between electrodes is small and the transit time is thus short. The nm scale of the device leads to a very high gain: typically 3000 electrons will recirculate during the hole lifetime.

Toward narrow band gap nanoplatelets

So far, most of the effort for the synthesis and optical investigation of 2D nanocrystal has been focused on cadmium and lead chalcogenides (PbX). PbX presents a narrower bulk band gap and is an interesting material to push the absorption toward the near infrared range. However, for this material the growth mechanism of the NPL is due to self-assembly of pre-formed nanocrystals and the absence of roughness obtained with CdSe has not been achieved yet by using PbX material.

We were very interested in demonstrating the synthesis of 2D nanoplatelets with narrow optical feature in the infrared. HgX compounds [34] as II-VI materials are more likely to generate a similar growth mechanism as the one observed for cadmium chalcogenides. Recently, HgX materials [35,36] has generated a lot of interest in the field of nanocrystal based optoelectronics for the design of low cost infrared [37,38] photodetectors [39,40,41].

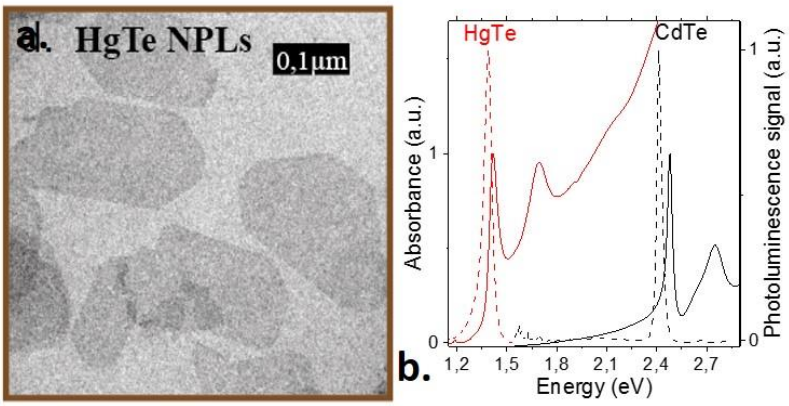

Figure 3 TEM image of HgTe NPL. b. Absorption and photoluminescence spectrum of CdTe and HgTe NPL.

Attempt for a direct synthesis of HgX NPL without surface roughness has so far been unsuccessful. We choose an indirect path by first synthetizing CdSe or CdTe NPL and then exchange the Cd for Hg cations. To preserve the 2D morphology and prevent a shape reconstruction, a bulky precursor of mercury has to be used. We typically prepare a mercury oleylamine complex and expose the NPL to this solution [42].

We observe a redshift of the spectrum over one hour, see Figure 3b. The final exciton appears between 800 and 900 nm and the 2D shape is preserved according to the TEM image, see Figure 3a. Because HgTe is a semimetal under bulk form, this means that the confinement energy is equal to the band edge energy and is almost equal to 1.5 eV, which is one of the strongest value reported so far. The key interest for this

material comes from the fact that the narrow character of the optical feature is preserved and the full width at half maximum of the PL is around 60 meV for an emission around 880 nm. This is typically twice narrower than what can be achieved with PbS or CIGS nanocrystals emitting at the same wavelength.

Finally, we investigate the transport properties of the HgTe NPL film [43]. Two capping ligands have been tested: EDT (1,2 ethanedithiol) and S^{2-} and both lead to conductive film. However their behaviors once used as channel of a field effect transistor are strongly different: EDT material presents a *p*-type character (*ie* rise of the conductance under hole injection), while the S^{2-} capping leads to n behavior (*ie* rise of conductance under electron injection), see Figure 4a and b.

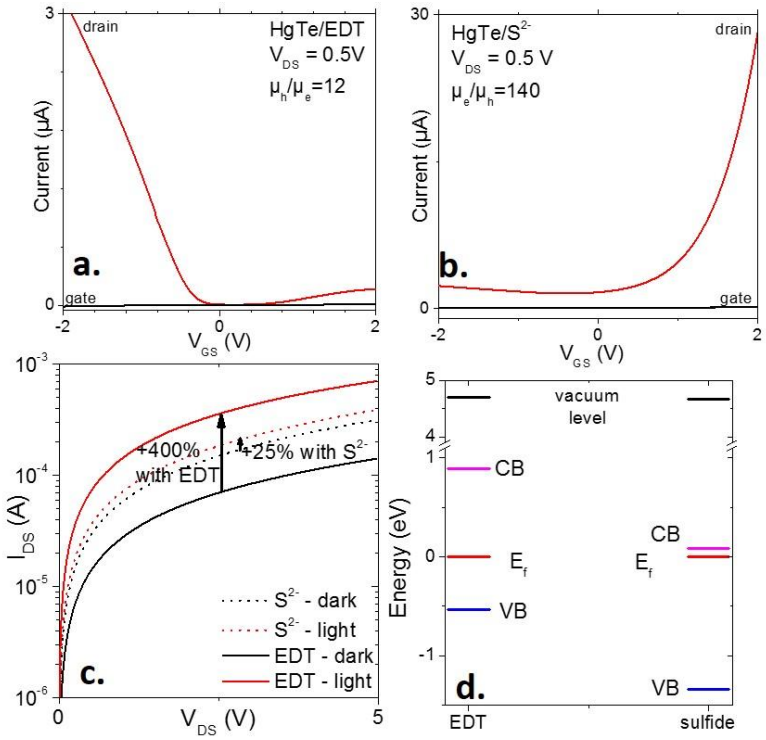

Figure 4Transfer curve for HgTe NPL capped with ethanedithiol (a) or sulfide ions (b). c: IV curve for the HgTe NPL capped with ethanedithiol or sulfide ions under dark condition or under illumination. Illumination is obtained from a 808 nm diode. d: Electronic spectrum in absolute energy scale of HgTe NPL capped with ethanedithiol or sulfide ions. All measurements are made at room temperature.

The photoconductive behavior of the two films also strongly differs from one ligand to the other. With EDT, the current modulation is large (x5). For the same illumination power, the sulfide leads to a very limited change in the current magnitude (+25%), see Figure 4c.

To understand the difference of behavior with the capping ligand we conduct photoemission measurements on the Tempo beamline of synchrotron Soleil. Our goal is to reconstruct in absolute energy scale the electronic spectrum of the two materials. Photoemission gives us information on the work function value (Fermi level *vs* vacuum) and relative position of the valence band with respect to the Fermi

level. If we add the band gap value obtained from PL measurement we are able to locate the vacuum level, as well as the valence and conduction band *vs* the Fermi energy. In this system, the vacuum level is the same for the two materials which means that the change of dipole associated with the two ligands is not leading to a significant surface band bending, in contrast to what can be observed for PbS [44] or HgSe [45] nanocrystals. For EDT, we observe that the Fermi level is located roughly in the middle of the gap, while with sulfide, the Fermi level is almost resonant with the conduction band leading to a more n type behavior. We attribute this shift of the band with respect to the Fermi energy to the formation of an HgS layer at the surface of the S^{2-} capped NPL. HgS is known as a self *n*-doped material [46] and this layer leads to the observed reinforcement of the *n*-doping over the whole NPL. This shift of the band are also fully consistent with transport experiment where the EDT material with p type doping leads to hole conduction while the sulfide capping, where the Fermi level is resonant with the conduction band only displays electron conduction. Also the reduction of photoconduction in the case of sulfide can be fully attributed to the rise of carrier density due to the degenerate character of the doping For HgTe/S^{2-}.

Conclusion

To conclude, we have investigated the transport and phototransport properties of CdSe/CdS NPL and HgTe NPL. A key difference compared with 0D object comes from the large exciton binding energy of the 2D material which needs to be addressed. Their anisotropic shape also leads to new device design possibility with a higher ease to connect single object or at least to conduct measurement at the single particle scale. Finally, we demonstrate that well controlled optical features are no longer limited to cadmium chalcogenides and that HgX compounds also present sharp transition, now in the infrared range.

Acknowledgments

We thank Agence Nationale de la Recherche for funding through grant Nanodose and H2DH. This work was supported by French state funds managed by the ANR within the Investissements d'Avenir programme under reference ANR-11-IDEX-0004-02, and more specifically within the framework of the Cluster of Excellence MATISSE. This work has been supported by the Region Ile-de-France in the framework of DIM Nano-K through the grant dopQD. EL thanks the support ERC starting grant through the project blackQD.

References

[1] M. Nasilowski, B. Mahler, E. Lhuillier, S. Ithurria, and B. Dubertret, Chem. Rev. **116**, 10934−10982 (2016).

[2] E. Lhuillier, S. Pedetti, S. Ithurria, B. Nadal, H. Heuclin, and B. Dubertret, Accounts for chemical research **22**, 48 (2015).
[3] Y. H Liu, V. L. Wayman, P.C. Gibbons, R. A. Loomis, and W. E. Buhro, Nano Lett. **10** (1), 352–357 (2010).
[4] J. S. Son, J. H. Yu, S. G. Kwon, J. Lee, J. Joo and T. Hyeon, Adv. Mater. **23** (28), 3214–3219 (2011)**.**
[5] J. Joo, J. S. Son, S. G. Kwon, J. H. Yu, and T. Hyeon, J. Am. Chem. Soc*.* **128** (17), 5632–5633 (2006).
[6] A. H. Khan, R. Brescia, A. Polovitsyn, I. Angeloni, B. Martín-García, and I. Moreels, Chem. Mater. **29** (7), 2883-2889 (2017).
[7] C. Schliehe, B. H. Juarez, M. Pelletier, S. Jander, D. Greshnykh, M. Nagel, A. Meyer, S. Foerster, A. Kornowski, C. Klinke, and H. Weller, Science **329** (5991), 550-553 (2010).
[8] J. Lauth, F. E. S. Gorris, M. S. Khoshkhoo, T. Chassé, W. Friedrich, V. Lebedeva, A. Meyer, C. Klinke, A. Kornowski, M. Scheele, and H. Weller, Chem. Mater. **28**, 1728-1736 (2016).
[9] W. J. Mir, M. Jagadeeswararao, S. Das, and A. Nag, ACS Energy Lett. **2** (3), 537–543 (2017).
[10] A. Riedinger, F. D. Ott, A. Mule, S. Mazzotti, P. N. Knüsel, S. J. P. Kress, F. Prins, S. C. Erwin, D. J Norris, Nature Mater. (2017).
[11] B. Mahler, B. Nadal, C. Bouet, G. Patriarche, and B. Dubertret, J. Am. Chem. Soc*.* **134** (45), 18591–18598 (2012).
[12] S. Ithurria, D. V. Talapin, J. Am. Chem. Soc. **134** (45), 18585–18590 (2012).
[13] A. V. Prudnikau, A. Chuvilin, and M. V. Artemyev, J. Am. Chem. Soc*.* **135** (39), 14476–14479 (2013).
[14] A. V. Antanovich, A. V. Prudnikau, D. Melnikau, Y. P. Rakovich, A. Chuvilin, U. Woggon, A. W. Achtstein, M. V. Artemyev, Nanoscale **7** (17), 8084-8092 (2015).
[15] I. Suarez, R. Munoz-Marmol, J. Martinez-Pastor, M. Artemyev, A. V. Prudnikau, A. V. Antanovich, A. Mikhailov, IEEE J. Selec. Top Quantum Elec. (2017)
[16] R. D Schaller, C.She, I Fedin, D. S Dolzhnikov, A. Demortière, R. D. Schaller, M. Pelton, and D. V. Talapin, Nano Lett. **14** (5), 2772–2777 (2014).
[17] J. Q. Grim, S. Christodoulou, F. Di Stasio, R. Krahne, R. Cingolani, L. Manna, and I. Moreels, Nature Nanotechnol. **9** (11), 891-895 (2014).
[18] B. Guzelturk, Y. Kelestemur, M. Olutas, S. Delikanli, and H. V. Demir, ACS Nano **8** (7), 6599–6605 (2014).
[19] S. Dogan, T. Bielewicz, Y. Cai, and C. Klinke, Appl. Phys. Lett. **101** (7), 073102 (2012)
[20] T. Bielewicz, S. Dogan, and C. Klinke, Small **11**, 826 (2015)
[21] B. Mahler, L. Guillemot, L. Bossard-Giannesini, S. Ithurria, D. Pierucci, A. Ouerghi, G. Patriarche, R. Benbalagh, E. Lacaze, F. Rochet, and E. Lhuillier, J. Phys. Chem. C **120**, 12351-12361 (2016).
[22] A. Nag, M. V. Kovalenko, J. S. Lee, W. Liu, B. Spokoyny, and D. V. Talapin, J. Am. Chem. Soc. **133** (27), 10612-10620 (2011)
[23] E. Lhuillier, A. Robin, S. Ithurria, H. Aubin, and B. Dubertret, Nano Lett. **14**, 2715-2719 (2014).
[24] S. Pedetti, B. Nadal, E. Lhuillier, B. Mahler, C. Bouet, B. Abécassis, X. Xu, and B. Dubertret, Chem. Mater. **25**, 2455 (2013).
[25] P. Guyot-Sionnest, E. Lhuillier, and H. Liu, J. Chem. Phys. **137**, 154704 (2012).
[26] E. Lhuillier, S. Pedetti , S. Ithurria, H. Heuclin, B. Nadal, A. Robin, G. Patriarche , N. Lequeux and B. Dubertret, ACS Nano **8**, 3813 (2014).
[27] E.Lhuillier, S. Ithurria, A. Descamps-Mandine, T. Douillard, R. Castaing, X.Z. Xu, P-L. Taberna, P. Simon, H. Aubin, and B. Dubertret, J. Phys. Chem. C **119**, 21795 (2015).
[28] E. Lhuillier, M. Scarafagio, P. Hease, B. Nadal, H. Aubin, X. Z. Xu, N. Lequeux, G. Patriache, S. Ithurria, and B. Dubertret, Nano Lett. **16**, 1282-1286 (2016).
[29] H. Cruguel, C. Livache, B. Martinez, S. Pedetti, D. Pierruci, E. Izquierdo, M. Dufour, S. Ithurria, H. Aubin, A. Ouerghi, E. Lacaze, M. G. Silly, B. Dubertret, and E. Lhuillier, Appl. Phys Lett. **110**, 152103 (2017).
[30] A. Robin, E. Lhuillier, X. Z. Xu, S. Ithurria, H. Aubin, A. Ouerghi, and B. Dubertret, Sci. Rep. **6**, 24909 (2016).
[31] A. W. Achtstein, A. Schliwa, A. V. Prudnikau, M. Hardzei, M. V. Artemyev, C. Thomsen, and U. Woggon, Nano Lett., **12** (6), 3151–3157 (2012).
[32] R. Benchamekh, N. A. Gippius, J. Even, M. O. Nestoklon, J. M. Jancu, S. Ithurria, B. Dubertret, A. L. Efros, and P. Voisin. Phys. Rev. B, **89** (3), 035307 (2014).

[33] E. Lhuillier, J.F. Dayen, D. O. Thomas, A. Robin, B. Doudin, and B. Dubertret, Nano Lett. **15**, 1736-1742 (2015).
[34] E. Lhuillier, S. Keuleyan, H Liu and P. Guyot-Sionnest, Chem. Mater. **25**, 1272 (2013).
[35] E. Lhuillier, and P. Guyot Sionnest, IEEE J. Selec. Top Quantum Elec. (2017).
[36] S. Keuleyan, E. Lhuillier, V. Brajuskovic, and P. Guyot-Sionnest, Nature Photon. **5**, 489-493 (2011).
[37] S. V. Kershaw, A. S. Susha, and A. L. Rogach, Chem. Soc. Rev. **42**, 3033, (2013).
[38] E. Lhuillier, S. Keuleyan, and P. Guyot-Sionnest, Nanotechnology **23**, 175705 (2012).
[39] X. Tang, X. Tang, and K. W. Chiu Lai , ACS Photonics **3**, 2396-2404 (2016).
[40] P. Guyot-Sionnest, and J. A. Roberts, Appl. Phys. Lett. **107** (25), 253104 (2015).
[41] E. Lhuillier, S. Keuleyan, P. Zolotavin, and P. Guyot-Sionnest, Adv. Mater. **25**, 137 (2013).
[42] E. Izquierdo, A. Robin, S. Keuleyan, N. Lequeux, E. Lhuillier, and S. Ithurria, J. Am. Chem. Soc. **138**, 10496 (2016).
[43] C. Livache, E. Izquierdo, B. Martinez, M. Dufour, D. Pierucci, H . Cruguel, L. Becerra, J.L. Fave, H . Aubin, A. Ouerghi, E. Lacaze, M. G. Silly, B. Dubertret, S. Ithurria and E. Lhuillier, Nano Lett **17**, 4067 (2017).
[44] P. R. Brown, D. Kim, R. R. Lunt, N. Zhao, M. G. Bawendi, J. C. Grossman, and V. Bulović, ACS Nano **8**, 5863–5872 (2014).
[45] A. Robin, C. Livache, S. Ithurria, E. Lacaze, B. Dubertret, E. Lhuillier, ACS Appl. Mat. Interfaces **8**, 27122−27128 (2016).
[46] G. Shen, and P. Guyot-Sionnest, J. Phys. Chem. C **120** (21), 11744-11753 (2016).